Sains Malaysiana 48(6)(2019): 1209–1219
http://dx.doi.org/10.17576/jsm-2019-4806-08

Effect of Synthesis Condition on the Structural Features of Ni-Ce Bimetallic Catalysts Supported on Functionalized Multi-Walled Carbon Nanotubes

(Kesan Daripada Keadaan Sintesis Pada Ciri-Ciri Struktur Ni-Ce Pemangkin Dwilogam Disokong oleh Berbilang-Fungsi Dinding Karbon Nanotiub)

NUR SYAHIDAH AFANDI, MEHRNOUSH KHAVARIAN & ABDUL RAHMAN MOHAMED*

ABSTRACT

In this paper, screening study in regards to preparation of functionalized multi-walled carbon nanotubes (FMWNT)-supported bi-metallic catalyst is discussed. Functional groups such as hydroxyl and carboxylic acid are introduced on multi-walled carbon nanotubes (MWCNT) surface using acid treatment method with the aid of probe-type ultrasonication. It is done by varying the concentration of nitric acid (HNO_3) and sulphuric acid (H_2SO_4), acid volume ratio and treatment duration. Catalysts with different ratios of cerium and nickel nanoparticles which are either loaded inside or outside of MWCNT were prepared via ultrasonic-assisted co-precipitation method (NiCe/CNT). This is done to study the effect of cerium loadings. The characterization of the FMWNT and catalysts are carried out using transmission electron micrographs (TEM), Fourier transform infrared spectroscopy (FTIR), thermogravimetric analysis (TGA), Brunauer-Emmett-Teller (BET), X-ray diffraction (XRD), and Raman spectroscopy. The results showed that the treatment in concentrated HNO_3/H_2SO_4 with volume ratio of 3:1 for 8 h was the most suitable condition to generate large amount of surface oxygen group with minimal defects. The observations for each used condition were discussed thoroughly. Decoration of MWCNT with different metal loadings resulted in different distribution and dispersion of metal on nanotubes surface.

Keywords: Functionalization; metal loading; multiwall carbon nanotubes; nickel-cerium based catalyst; ultrasonication

ABSTRAK

Dalam kertas ini, kajian saringan berkaitan dengan penyediaan pemangkin pemfungsian nanotiub karbon berbilang dinding (FMWNT) yang menyokong dua logam dibincangkan. Kumpulan fungsian seperti hidroksil dan asid karboksilik diperkenalkan pada permukaan tiub nano karbon berbilang dinding (MWCNT) menggunakan kaedah rawatan asid dengan bantuan ultrasonik jenis probe. Ia dilakukan dengan menvariasikan kepekatan asid nitrik (HNO_3) dan asid sulfurik (H_2SO_4), nisbah isi padu asid dan tempoh uji kaji dijalankan. Pemangkin dengan nisbah zarah nano cerium dan nikel yang berbeza yang sama ada dimuatkan di dalam atau di luar MWCNT telah disediakan melalui kaedah pemendakan yang dibantu ultrasonik (NiCe/CNT). Ia dijalankan untuk mengkaji kesan muatan cerium. Pencirian FMWNT dan pemangkin ditentukan dengan menggunakan mikroskop elektron penghantaran (TEM), spektroskopi inframerah transformasi Fourier (FTIR), penganalisis termogravimetri (TGA), pencirian kawasan permukaan (BET), spektrometer pembelauan sinar-X (XRD) dan spektroskopi Raman. Keputusan menunjukkan bahawa rawatan dalam HNO_3/H_2SO_4 yang pekat dengan nisbah isi padu asid 3:1 selama 8 jam adalah keadaan yang paling sesuai untuk menghasilkan banyak kumpulan oksigen dengan kecacatan yang minimum. Pemerhatian bagi setiap keadaan yang digunakan dibincangkan dengan teliti. Penghiasan FMWNT dengan muatan logam yang berbeza mengakibatkan pengagihan dan penyebaran logam yang berbeza pada permukaan tiub nano.

Kata kunci: Fungsian; muatan logam; pemangkin berasaskan nikel - cerium; tiub nano karbon berbilang dinding; ultrasonikasi

INTRODUCTION

For over two decades, carbon nanotubes (CNTs) have been subjected to research works inspired based on materials science and technology revolution. Hollow cylinders of CNTs which are fabricated from rolled-up sp^2 graphene layers is undoubtedly considered to be a special nanomaterial that offers fascinating properties such as large surface area, well-defined structures, functionalizable surfaces, excellent electronic with unique transport properties (Zhou et al. 2017). These outstanding properties have evoked growing interest in heterogeneous catalysis production and it has been regarded as a powerful catalyst support. However, owning to their novelty in chemical inertness and deep-rooted hydrophobicity achieving homogeneous solubility and dispersion of CNTs in polar liquids still remain a major drawback (Kuroda et al. 2016). Moreover, the nature of the as-synthesized CNTs which tend to entangle together as bundles and ropes dominates their high surface energy and strong van der Waals interaction (Tatsuru et al. 2013). This kind of restrictions adversely

affects the available active sites and thus the dispersion of uniform size of nanoparticles inside and outside the CNTs is very limited.

It is worth noting that chemical modification called functionalization is a promising means that can be used to modify the graphitic surface to encounter the growing demand. Functionalization aims to alter the surface chemistry of CNTs from sp^2 to sp^3 hybridization leading to the formation of various oxygen-containing functional groups at the sidewalls and open-ended CNTs (Kharissova et al. 2013). The Covalent's approach is one of the simple ways and more preferred ones as it has several advantages such as high stability, reproducibility, as well as better controllable number of functional groups without damaging their structure and properties a lot (Guo et al. 2017).

Normally oxygenated surface groups are present at the graphitic debris as amorphous fragments which are very reactive towards oxidation. In some cases, structural defects also will be present along the sidewall and act as prime sites during the functionalization process (Garzia et al. 2017). Therefore, a simple and effective strategy for producing novel functionalization routes are needed as prerequisite to promote the increment of carboxylated groups on the internal and external surface of nanotubes. In general, MWCNT were suspended in mixture of HNO_3 and H_2SO_4 under probe-type ultrasonication for 5 min to deliver shear stress for dispersing aggregates and are also subsequently refluxed over certain duration. There is a high motivation to apply probe-type ultrasonication since ultrasound irradiation activates the carbon-carbon bonds, and then accelerate the chemical reactions for the introduction of functional groups (Le et al. 2017). Probe-type ultrasonication is a useful tool to achieve better dispersion in aqueous solution compared to ultrasonic water bath due to the uniform ultrasonic irradiation. Although functionalization had been reported by few researchers previously, there is still a lack of methodical study on the effect of acid volume ratio, different acid molarity, and concentration of oxygen groups. Herein, a series of covalently FMWNT were developed to investigate the nature of MWCNT subjected to different degree of oxidation as an addition to prevail available data.

To date, many researchers have endeavored in decorating metals nanoparticles on FMWNT for variety of applications such as syngas conversion (Liu et al. 2014), photocatalysis (Azqhandi et al. 2017), NH_3 decomposition (Bell et al. 2017), and hydrogenation of alkynes (Wang et al. 2017). Such surface groups that are grafted can provide sites for cation nanoparticles attachment which causes a good electrical contact for FMWNT with metal particles. In the present work, attachment of bimetallic Ni-Ce nanoparticles on FMWNT with certain range of Ce loading are prepared by ultrasonic-assisted co-precipitation method to investigate the effect of bimetallic loading in details. The catalysts are characterized using various analytical methods to understand the nature of metal particles and CNTs support as well as their interactions.

Materials and Methods

Functionalization Method

MWCNT were synthesized using catalytic chemical vapor deposition process with Co-Mo/MgO catalyst. The MWCNT had specific outer diameter of 10-20 nm, inner diameter of 4-8 nm, length of 5-20 μm with purity greater than 99%. Considering the fact that functional groups are more likely to occur first at the debris and structural defects (Tessonnier et al. 2009), a very high purity MWCNT was utilized to reduce those troublemaking aspects. In a typical experiment, 1 g of MWCNT was suspended in a mixture of 100 mL HNO_3/H_2SO_4. Prior to the process, the solution was sonicated by probe-type ultrasonication for 5 min (Fisher Scientific, FB120) at room temperature and then refluxed at 100°C under moderate stirring (200 rpm) in a Soxhlet apparatus. After filtering, the product was dried overnight in an oven at 110°C. Functionalization of MWCNT was performed via oxidation with different volume ratio of HNO_3:H_2SO_4 (3:1, 1:3 and 1:1), different concentrations of HNO_3/H_2SO_4 mixture (8 M, 9 M, 10 M and using concentrated HNO_3 (68%) and H_2SO_4 (98%)) at different treatment duration of 2, 4, 8, 16 and 24 h. Herein, the functionalized samples were coded as FMWNT (volume ratio, molarity, time).

Ni-Ce Supported FMWNT Preparation

The Ni-Ce supported FMWNT catalyst was prepared via ultrasonic-assisted co-precipitation method. FMWNT was added into 50 mL $Ce(NO_3)_3 \cdot 6H_2O$ and $Ni(NO_3)_3 \cdot 9H_2O$ aqueous solution containing deionized water and stirred for 1 h. The resulting slurry was sonicated for 30 min. Then, 1 M of NaOH droplets were added with vigorous stirring until pH11 was achieved. After that, the mixture was aged for 4 h at room temperature. Finally, the formed precipitate was filtered and dried at 100°C overnight. The resulting solid mixture was calcined at 500°C in N_2 stream for 4 h at a rate of 5°C/min to obtain Ni-Ce/CNT.

To evaluate the effects of metal ratio on the catalyst structural properties, the NiCe/CNT with different ceria loadings (x) of 5, 10, 15, 20, 30, and 50% were synthesized. The nickel loading was fixed at 5% in all catalyst unless stated otherwise. The catalysts were labelled as Ni_5Cex/CNT for catalyst with different ceria loadings (x).

Results and Discussion

Characterization of FMWNT

Morphology The microstructures of as-synthesized and functionalized MWCNT with various parameters were investigated using TEM. Figure 1(a) represents the TEM image of as-synthesized MWCNT with closed end caps where the tubes entanglement can be observed with a few scattered metal nanoparticles encapsulated inside the channels. Meanwhile, Figure 1(b)-1(f) shows the

TEM images of the FMWNT with different acid volumes as well as different acid concentrations. No impurities such as catalyst particles and disorder carbon along the surface after oxidation were observed. Besides that, it is observed that there was no major discrepancy in the structure of MWCNT before and after acid treatment. This indicated that the vibration from ultrasonic treatment did not cause damage or fracture to individual nanotubes. As shown in Figure 1(b)-1(d) and 1(f), it can be seen that the nanotube structure of the FMWNT did not suffer from breakage. This result shows that it is suitable to use acid mixture of 9 M, 10 M, and concentrated acid volume with ratio of 3:1 and 1:1 for the functionalization of MWCNT with the aid of ultrasonication. The aggregation of the nanotubes due to the cavitation can be exfoliated by the strong shear force produced from ultrasound vibration where the process starts with bubble formation, growth, and then collapses. For FMWNT (1:3, concentrated, 8 h), breakage point (marked by red circle in Figure 1(e)) and surface roughness can be observed. Increase of the amount of H_2SO_4 during functionalization increases the $-OSO_3H$ groups in the final product. It is believed that more defects are created to the hexagonal and pentagonal structures when the concentrations of NO_2^- which is responsible for attacking to aromatic compounds and $-OSO_3H$ which is a strong protonic acid group increase due to the use of concentrated acid; this is in agreement with other findings previously (Kanbur & Küçükyavuz 2011).

Figure 1(g)-1(i) illustrates the TEM images of FMWNT with different treatment time of concentrated HNO_3/H_2SO_4 with volume ratio of 3:1. From Figure 1(g)-1(h), where the oxidative duration was for 2 h and 4 h, the sidewall surface was still coated with a thin layer of amorphous carbon. This implies that the duration was just enough to eliminate the carbon disorder without causing damage to the nanotubes. The prolonged treatment duration diminishes the level of amorphous carbon. However, during this experiment, some sidewall damages occurred too as a result of functional groups attachment. The outermost graphene sheets were evidenced to be distorted in the linearity when the oxidation was for 16 h and this led to a significant increase in the amount of open ends due to the hexagon electrophilic attack by HNO_3/H_2SO_4 (Chiang et al. 2011).

FTIR Figure 2 shows the FT-IR spectroscopy of pristine MWCNT and FMWNT treated using different HNO_3/H_2SO_4 concentration and different volume ratio for 8 h. The FTIR spectrums of all samples showed two distinct bands, located at 3450 cm^{-1} and 1634.5 cm^{-1}, respectively. The band at 3450 cm^{-1} could be assigned to the hydroxyl group (-OH) stretching from the carboxylic acid and phenol groups, while the band at 1634.5 cm^{-1} could be identified

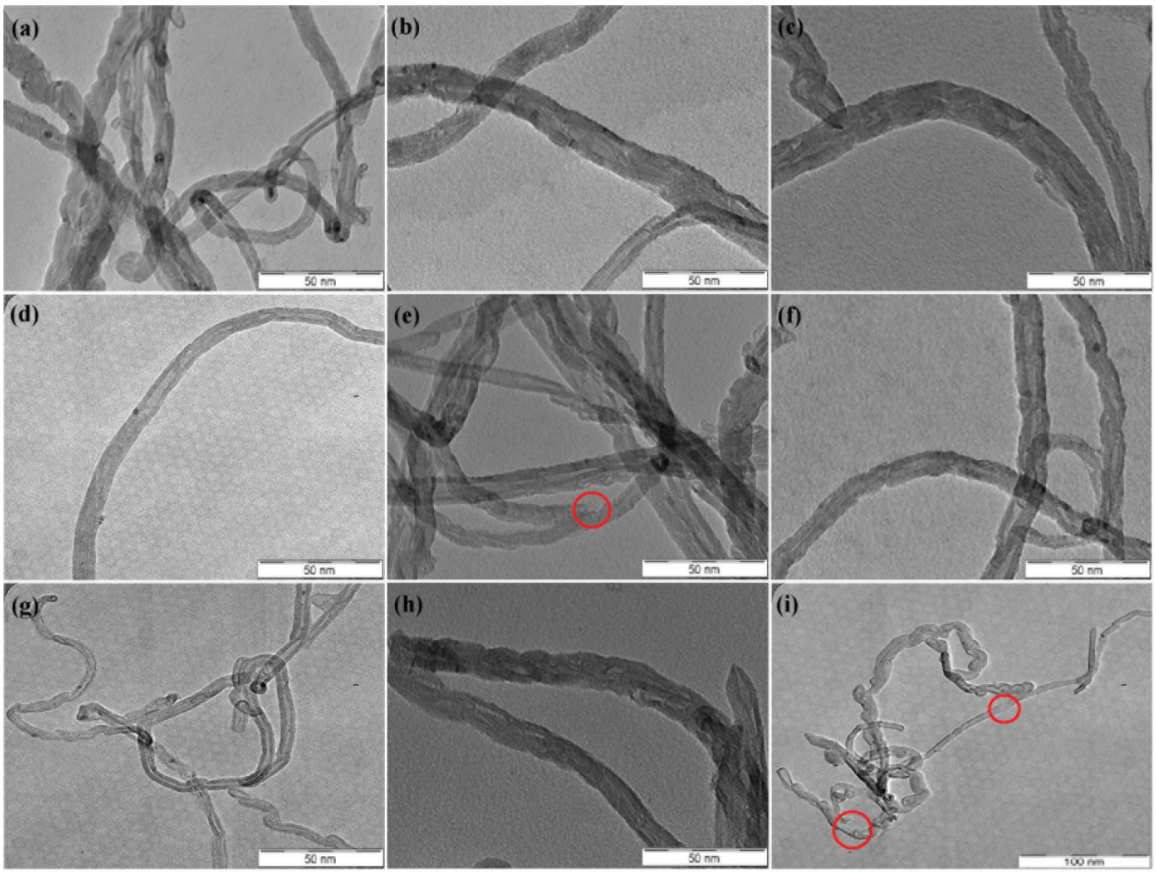

FIGURE 1. TEM image: (a) as-synthesized MWCNT; (b) FMWNT (3:1, 9 M, 8 h); (c) FMWNT (3:1, 10 M, 8 h); (d) FMWNT (3:1, concentrated, 8 h); (e) FMWNT (1:3, concentrated, 8 h); (f) FMWNT (1:1, concentrated, 8 h); (g) FMWNT (3:1, concentrated, 2 h); (h) FMWNT (3:1, concentrated, 4 h); and (i) FMWNT (3:1, concentrated, 16 h)

as the carbonyl (C=O) absorption band, overlapped with the (C=C) (Morsy et al. 2014). The (C=C) represents the backbone the CNTs structure (Gui et al. 2013). On the other hand, the carbonyl (C=O) band stretching may be contributed by the carboxyl group (–COOH) attached on the surface of CNTs. The small peak observed around 2370 cm^{-1} is ascribed to -OH stretching from H-bond-COOH (Abuilaiwi et al. 2013).

The broadening of both 3450 cm^{-1} and 1634.5 cm^{-1} peaks decreases in a sequence of pristine MWCNT< FMWNT (3:1, 8 M, 8 h) < FMWNT (3:1, 9 M, 8 h) < FMWNT (3:1, 10 M, 8 h) < FMWNT (3:1, concentrated, 8 h) < FMWNT (1:1, concentrated, 8 h) < FMWNT (1:3, concentrated, 8 h). This suggested that the concentration of carboxylic acid moieties at the internal and external surface of FMWNT and it increases with the increase in concentration of HNO_3 and H_2SO_4. Besides that, the ultrasound vibration also promotes the interface interactions of the nanotubes in acid solutions by breaking the agglomeration parts to earn a fine dispersion condition. The intensity of both peaks increased more when FMWNT (1:3, concentrated, 8 h) was used compared to when the volume ratio of 3:1 and 1:1 were used, indicating that the effect of increasing sulfuric acid concentration is more pronounced due to the higher oxidation power of sulfuric acid. In addition, it is also found that the both peaks broadened with increase of acid treatment time.

Abundant of oxygenated functional groups were present on FMWNT surface and it can provide a large amount of active sites that increase the ion exchange capacity for metal attachment. This is because, increasing amounts of acidic groups like carboxylic acid increases the hydrophilicity of FMWNT. Meanwhile, increasing amounts of basic groups like carbonyl could improve the metals dispersion and affinity towards FMWNT.

RAMAN ANALYSIS

Figure 3 exhibits the resonance Raman spectra of the MWCNT and FMWNT for diverse acid ratios. There are three main peaks presented that were identified as the defect band (D-band) at around 1365 cm^{-1}, the graphitic structure (G-band) at around 1590 cm^{-1}, and the second-order region of graphitization (G'-band) at 2700 cm^{-1}. D-band is represented by the sp^3-hybridized MWCNT, disordering of the nanotubes and G-band is attributed to the sp^2-hybridized MWCNT (Ling et al. 2013). For pristine MWCNT, the intensity of the G-band is observed to be slightly higher than D-band (I_D/I_G = 0.98). This indicates that the pristine MWCNT has high graphitization of carbon that was contributed by the high purity of MWCNT. The I_D/I_G ratio of FMWNT (1:1, concentrated, 8 h), FMWNT (3:1, concentrated, 8 h) and FMWNT (1:3, concentrated, 8 h) are 1.03, 1.04, and 1.07, respectively. The increment of the I_D/I_G value is observed and is considered as an effect of the presence of more disorder in carbon as reported by the FTIR. This situation contributed to high degree of functionalization. However, upon being subjected to the harshest conditions, the defect sites became larger and it caused damage to the MWCNT surface as well as gives rise to shortening of the nanotubes (Gopiraman et al. 2013). This strong impact of the acid ratio of 1:3 on the defect sites is devoted to the strong oxidative treatment capabilities of sulphuric acid. In addition, the decrease in $I_{G'}/I_G$ and $I_{G'}/I_D$ value in FMWNT (1:3, concentrated, 8 h) indicated the roughness of nanotube walls as well as the poor crystallization quality.

On this basis, there are two common steps involved in the oxidation mechanism of the structural transformation of CNTs. Firstly, the oxidants attack the CNT sidewalls and generate some active sites such as –OH groups (Zhang et al. 2003). Here, the disordered carbon is removed

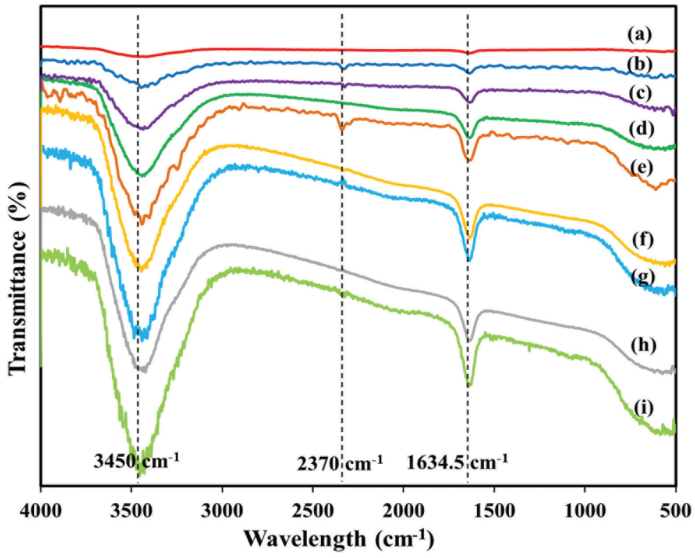

FIGURE 2. FTIR spectra of: (a) Pristine MWCNT; (b) FMWNT (3:1, 8 M, 8 h); (c) FMWNT (3:1, 9 M, 8 h); (d) FMWNT (3:1, 10 M, 8 h); (e) FMWNT (3:1, concentrated, 8 h); (f) FMWNT (1:1, concentrated, 8 h); (g) FMWNT (1:3, concentrated, 8 h); (h) FMWNT (3:1, concentrated, 16 h); and (i) FMWNT (3:1, concentrated, 24 h)

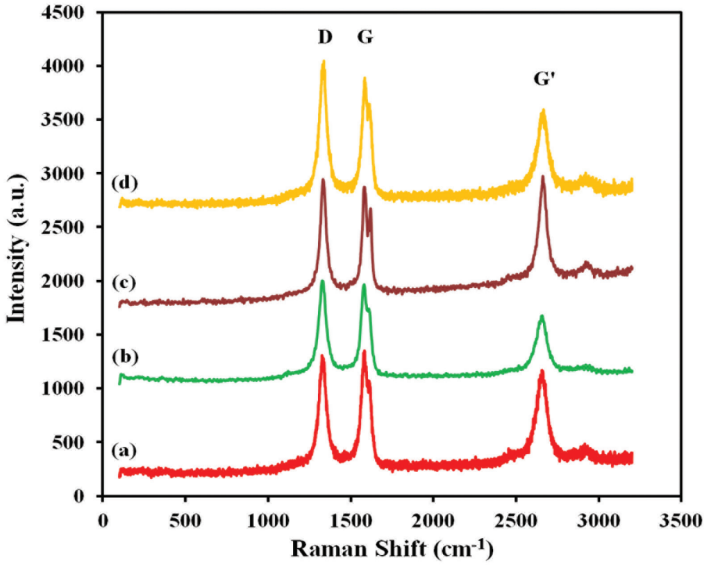

FIGURE 3. Raman spectra of (a) Pristine MWCNT; (b) FMWNT (1:1, concentrated, 8 h); (c) FMWNT (3:1, concentrated, 8 h); and (d) FMWNT (1:3, concentrated, 8 h)

without generation of any defect. After that, prolonging the oxidation treatment with aggressive condition leads to defect-generating step and defect-consuming step where the hexagon electrophilic attack occurs concurrently. Defect-generating step occurs rapidly than defect-consuming step and commits to creation of large amount of functional groups on FMWNT (Santangelo et al. 2012).

THERMAL STABILITY

TGA curves can be reported in regards to the weight loss of the material as a function of temperature. The initiation temperature and the oxidation temperature are the key parameters of a TGA curves (Lehman et al. 2011). The TGA analyses performed in flowing air on the FMWNT at different acid ratios and different treatment time are presented in Figure 4(a) and 4(b). From Figure 4(a), it can be seen that the initiation temperature and the oxidation temperature are slightly different for all the samples. Higher acid concentration resulted in lower initiation and oxidation temperatures. FMWNT (1:3, concentrated, 8 h) had the lowest initiation and oxidation temperatures of 511°C and 581°C, respectively. Thus, FMWNT with the highest concentration of H_2SO_4 exhibited the lowest thermal stability. More oxygenated functional groups were created on the FMWNT surface and its hexatomic ring structure was destructed as well where these results were further confirmed by TEM images (Ling et al. 2013). Furthermore, the weight loss decreased to less than 1% only for FMWNT (3:1, concentrated, 8h) and about 6% weight loss for the acid ratio of 1:3 and 1:1 was encountered. This indicates that the purity of FMWNT decreased by 6% when harsher acid is applied during the oxidative treatment. For the effect of different treatment time, the samples with longer acid treatment time have a lower initiation and oxidation temperatures due to the damage done to the outer surface. However, the oxidation temperature for oxidative treatment at 2 h and 4 h increases and this is attributed to the removal of debris and amorphous carbon. The existing active sites such as -CH_2 and -CH groups were also being attacked by the oxidant at an initial oxidation stage and remarked the slight improvement of thermal stability of the FMWNT (Sahebian et al. 2016). Besides that, the weight loss in the range between 350°C and 650°C may be explained by the degradation of anhydrides and lactones as well as the decomposition of carboxyl, carbonyl, quinone, and ether groups (Pistone et al. 2012).

From all the analysis, it can be concluded that acid ratio, acid concentration, and treatment time have significant effects on the decoration of MWCNT with functional groups. FMWNT (3:1, concentrated, 8 h) has been chosen for the attachment of bimetallic Ni-Ce nanoparticles on FMWNT surface. This particular oxidation condition satisfies the needs and it provided good results for all the characterizations evaluated such as it had high concentration of functional groups, the nanotubes structure remained the same after acid treatment, high acidic surface, high zeta potential value, and high stability.

EFFECT OF Ce LOADINGS ON THE DECORATION OF FMWCNT

The microstructures of NiCe/CNT with different Ce loading were investigated using TEM. Figure 5(a) – 5(f) shows the TEM images of NiCe/CNT coated with various cerium loadings which were 5, 10, 15, 20, 30, and 50%, respectively. The images show that all CNTs-based catalysts regardless of the cerium content are covered with nanoparticles. The average size of the Ni and Ce oxides is in the range of 3-30 nm. It can be clearly observed in Figure 5(a) and 5(b) that Ni and Ce nanoparticles were uniformly dispersed on the exterior surface of the CNTs. However, Figure 5(e) and 5(f) shows small amount of

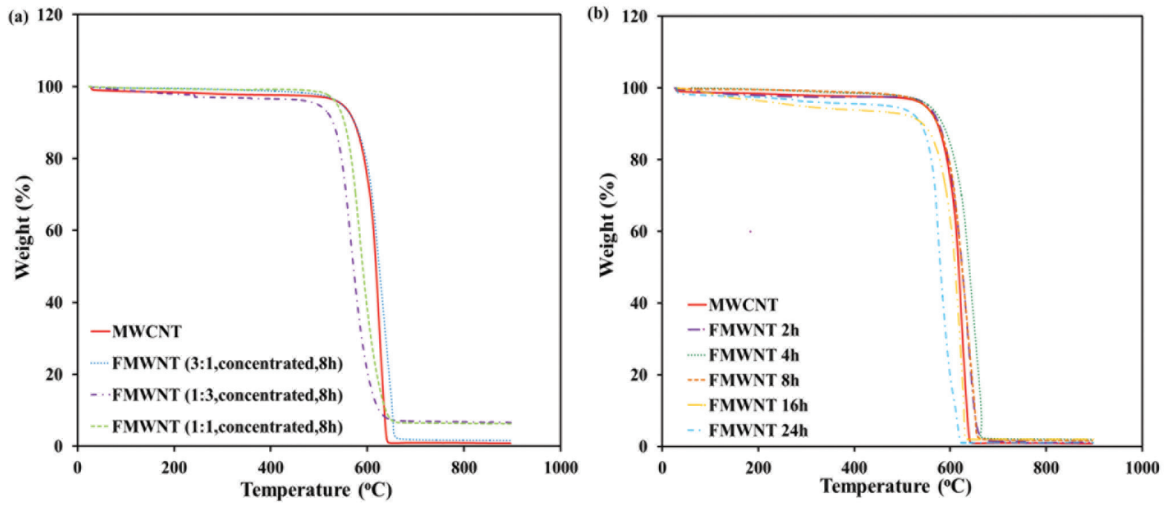

FIGURE 4. (a) TGA profile of FMWNT at different acid ratio; (b) TGA profile of FMWNT at different treatment time

Ni and Ce aggregates together where less distribution was observed in the catalyst with Ce loadings of 30 and 50%, respectively. This indicates that increment in the Ce content over the FMWNT resulted in increase of the cluster nanoparticles. In addition, it should be noted that the generated surface oxygenated sites or active sites from the oxidation treatment are same in all samples. Hence, the increase in nanoparticles agglomeration with increasing of Ce loading is assigned due to the saturation of the active sites which are available for metals deposition. The location of the nanoparticles whether outside or inside the CNTs cannot be clarified clearly due to the two dimension of TEM images.

Figure 6(a) – 6(f) shows the observed XRD patterns of NiCe/CNT for different Ce loadings. All catalysts exhibit two diffraction peaks at 26.3° and 42.5° which correspond to the (002) and (100) reflections of hexagonal graphite, respectively. This indicates that the graphitic structure was not destroyed even after undergoing harsh oxidation process and calcination at high temperature. The diffraction peaks of 2Θ centered at 44.3°, 51.8°, and 63° are assigned to the (111), (200), and (220) crystallographic plane of Ni, respectively. Meanwhile, the peaks at 28.5°, 32.9°, 48.6°, 56.6°, 69.7°, and 78.2° could be attributed to the Ce particles. It is found that the peaks of the catalysts that possess smaller amount of Ce loading are broader and weaker than the ones with the higher Ce content. This indicated that the Ni and Ce crystallites size are smaller for the catalysts with smaller amount of Ce loading. The crystallite size produced at different Ce loadings was calculated using Scherer's equation, giving the Ce particle size of 3.2, 7.1, 9.4, 11.3, 19.5, and 29.6 nm, accordingly. As can be seen from Figure 6(a), Ni_5Ce_5/CNT does not display any diffraction peaks of Ce because very small particles could not be detected by XRD. This could justify the fact that the Ce was well dispersed on the FMWNT under low Ce loading. Obvious peaks ascribed to the Ce crystalline phase which is higher than graphite peaks could be observed for Ni_5Ce_{50}/CNT. The raising intensities of Ce peaks implied that the aggregation of nanoparticles accompanied with the increment in Ce crystallite size, resulted in poor nanoparticles dispersion. Meanwhile, the decline in the intensity of graphite peaks implied that the structure of FMWNT had been disturbed due to the decoration of metals on their surface.

Figure 7(a) shows the TGA curves of NiCe/CNT used to examine the effect of Ce loading on the catalyst stability and also the dispersion of the nanoparticles on the CNTs surface. The results showed that the oxidation temperature of the NiCe/CNT for all metal loading shifted to a lower temperature due to the introduction of Ni and Ce nanoparticles. The weight loss rapidly started at temperatures below 200°C and it increased to a temperature below 400°C due to the presence of the displaceable water and counter ions in the catalyst. All the catalysts have a single oxidation step where nearly all nanotubes surface had been coated with Ni and Ce nanoparticles. Figure 7(b) shows the DTG curves of NiCe/CNT for different Ce loadings. It can be seen that at lower Ce loading of 5% and 10%, the oxidation of Ni_5Ce_5/CNT and Ni_5Ce_{10}/CNT took place at two different temperatures. This situation showed that the dispersion of Ni and Ce do not necessarily embrace the entire CNTs surface due to the lower metal loading. Although TEM and XRD results showed that great dispersion of nanoparticles at lower Ce loadings happened, but still some of the individual nanotubes surface remain uncovered by Ni and Ce during catalyst preparation which contributed to the non-uniform oxidation stages. Meanwhile, for higher Ce loading, it only has a single cracking temperature which centres around 490 and 470°C, respectively. It is anticipated that metals distribution increases within these range of metal loading. Increase in metal loadings caused the DTG graphs to shift to a lower temperature when compared to the other catalyst due to the abundance amount of metals presence.

The N_2 adsorption-desorption isotherms and the pore size distribution of the FMWNT and Ni_5Ce_x/CNT

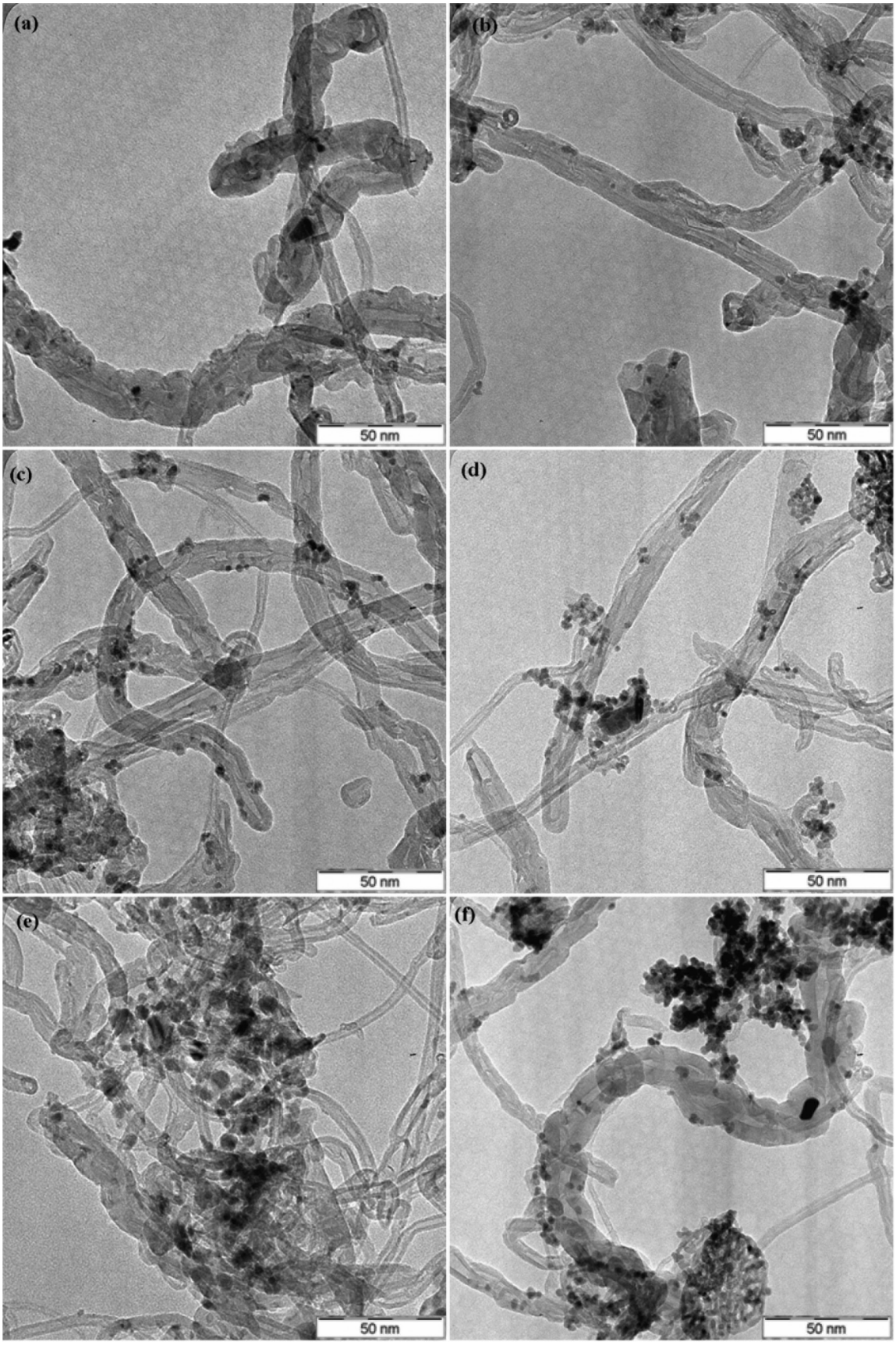

FIGURE 5. TEM images of (a) Ni_5Ce_5/CNT; (b) Ni_5Ce_{10}/CNT; (c) Ni_5Ce_{15}/CNT; (d) Ni_5Ce_{20}/CNT; (e) Ni_5Ce_{30}/CNT; and (f) Ni_5Ce_{50}/CNT

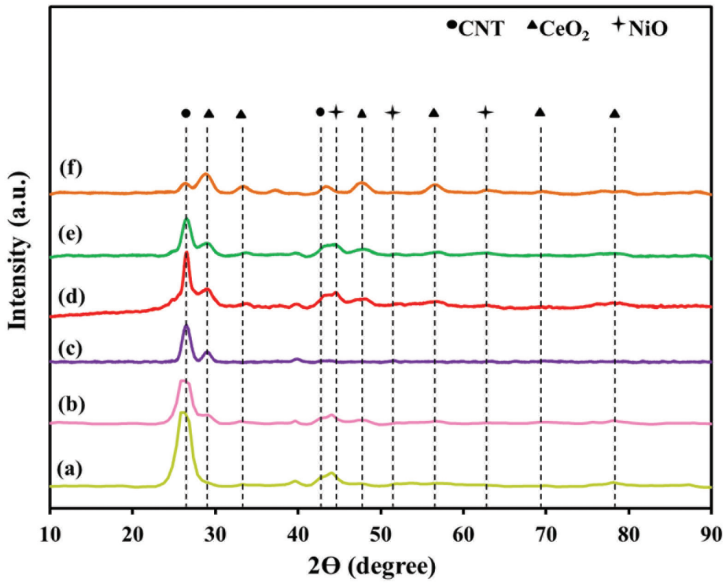

FIGURE 6. XRD patterns of (a) Ni_5Ce_5/CNT; (b) Ni_5Ce_{10}/CNT; (c) Ni_5Ce_{15}/CNT; (d) Ni_5Ce_{20}/CNT; (e) Ni_5Ce_{30}/CNT; and (f) Ni_5Ce_{50}/CNT

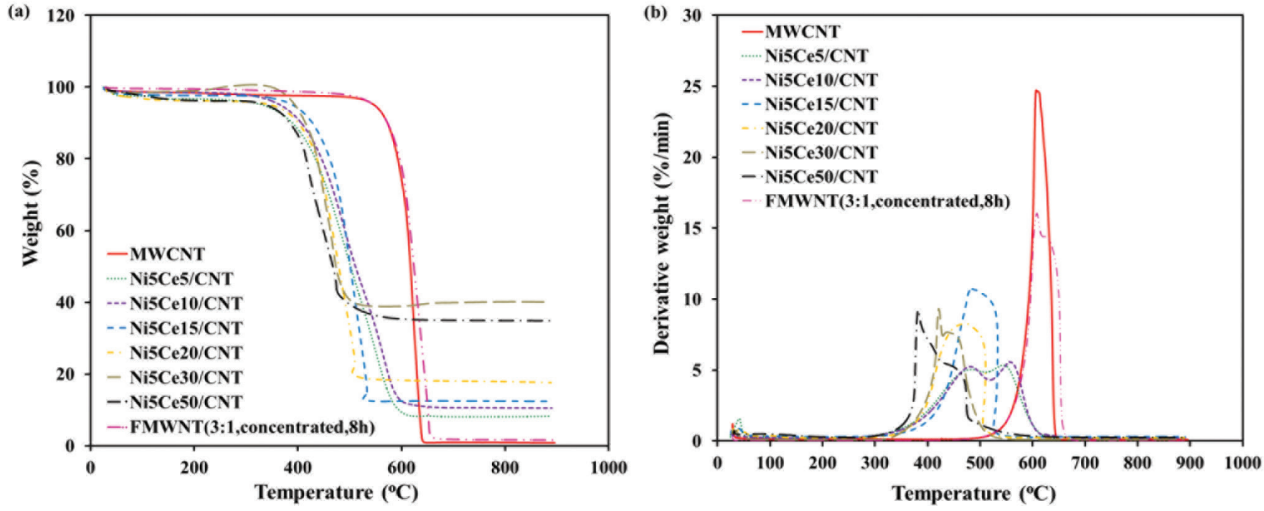

FIGURE 7. (a) TGA profile of NiCe/CNT at different Ce loading; and (b) DTG profile of NiCe/CNT at different Ce loadings

with different Ce loadings are illustrated in Figure 8(a) and 8(b). Based on the IUPAC classification, all the catalysts exhibited mesopore features as most of pore size distribution calculated by BJH formula fall in the range 3-4 nm. It clearly shows that small size distribution or internal cavity of the CNTs is decreased at Ce loading of 50%, which is attributed to the Ni and Ce particles that was filled in the pores that were available. The adsorption-desorption isotherms could be classified into type-IV that look like a hysteresis loops at higher relative pressure indicating the capillary condensation steps in mesopores (Xiao et al. 2016). A poor adsorption capability was implied by the adsorption isotherm at low pressure which is attributed to the few micropores available in the nanocomposite structure. However, the adsorption isotherm experiences a sharp increase when approaching P/Po = 1 suggesting the presence of mesopores and also some larger pores (Xiao et al. 2016). Meanwhile, the observed surface area increment along with the hysteresis loop on adsorption-desorption isotherm speculates a partial uncapping of the nanotubes as a result of oxidative treatment. Furthermore, the hysteresis loop which virtually disappear for Ni_5Ce_{50}/CNT happens due to the accumulation of Ni and Ce nanoparticles on the FMWNT channels where it reduces the pore size (Ma et al. 2013). Textural properties of FMWNT and NiCe/CNT catalysts are listed in Table 1. As can be seen, the BET surface area of Ni_5Ce_5/CNT and Ni_5Ce_{10}/CNT were higher than that of FMWNT. It may result in more defects being created on the FMWNT surface due to the sonication step applied during catalyst preparation, which causes carbon oxidation of FMWNT. It must be noted that high specific surface area can improve the catalytic activity of the catalyst by offering extra active sites. Continuing this, the

TABLE 1. The physical characteristics of the catalysts of different Ce loading

Catalysts	BET surface area ($m^2 g^{-1}$)	Pore volume ($cm^3 g^{-1}$)	Average pore diameter (nm)
FMWNT	145.2	0.586	16.1
Ni_5Ce_5/CNT	152.5	0.550	14.4
Ni_5Ce_{10}/CNT	158.9	0.579	14.5
Ni_5Ce_{30}/CNT	125.9	0.540	17.1
Ni_5Ce_{50}/CNT	124.4	0.476	15.3

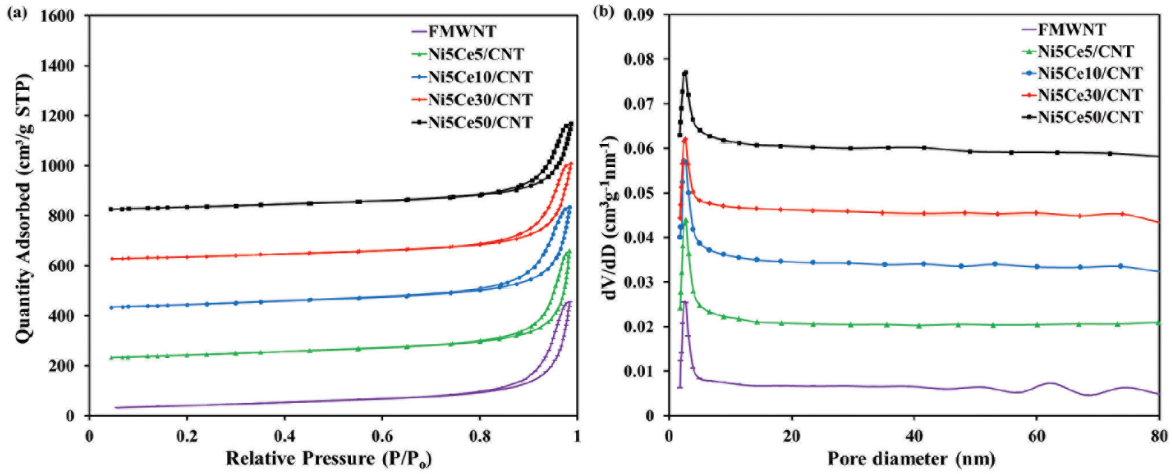

FIGURE 8. (a) Nitrogen adsorption-desorption isotherms; (b) Pore size distribution the catalysts

surface area and total pore volume decreased with further increment of Ce loading. The decrease in the surface area could indicate that some mesopores have been blocked by the excess Ni and Ce nanoparticles and it contributed to severe agglomeration on the nanotube channels.

The Ni and Ce attachment on FMWNT also depends on the adsorption mechanism in achieving good metal dispersion. It has been previously reported that chemical interaction is the major mechanism that is responsible for the metal loading. Due to this, the increase in surface total acidity and basicity are responsible for the interaction of cation ions in the aqueous solution (Ren et al. 2011). As for this case, functionalization treatment created many oxygenated functional groups such as OH^- and $COOH^-$, thus it reduces the hydrophobicity character of the carbon nanotubes and allow wetting with aqueous solutions containing Ni and Ce to take place.

CONCLUSION

In this study, different aspects of the effect of functionalization of MWCNT by HNO_3/H_2SO_4 acid were carried out to discuss on the structure and surface chemistry of MWCNT. The new active sites as well as oxygenated functional groups were created when the oxidant begins to attack the integrated MWCNT structure and the number of active sites increased as the treatment was prolonged. Raman spectroscopy results proved that crystallization quality decreased as compared to pristine MWCNT due to the attachment of functional groups which makes the surface roughness of MWCNT become more detected. The main groups created on the nanotube surface during functionalization process are mainly –OH and –COOH groups as explained in FTIR analysis. According to all analysis, it can be deduced that functionalization of MWCNT in concentrated HNO_3/H_2SO_4 for 8 h results in higher oxygenated functional groups to be created. The nanotube structure still remains the same and no breakage was found after the treatment. In addition, the effect of functionalization towards the decoration of bi-metallic nanoparticles on FMWNT was also explained. Based on the analysis results, it is observed that FMWNT (3:1, concentrated, 8 h) together with ultrasonic-assisted co-precipitation method can be successfully used for the formation of NiCe/CNT catalyst. The sonication step applied is believed to lead the Ni and Ce nanoparticles to be homogenously dispersed on the surface of FMWNT. The presence of oxygenated functional groups as a result of surface modification decreased the hydrophobic nature of FMWCNT and created a good interaction between Ni^{2+} and Ce^{3+} ions with nanotubes surface via electrostatic attraction. It was also found that the crystallite size increases as Ce loading was increased. The BET analysis explained that the surface area of FMWNT slightly increased with low metal loadings as a result of more defects being generated.

ACKNOWLEDGEMENTS

The authors thank the USM-NanoMITE Grant (LRGS): 203/PJKIMIA/6720009 for financial support.

REFERENCES

Abuilaiwi, F., Laoui, T., Al-Harthi, M. & Atieh, A. 2013. Modification and functionalization of multiwalled carbon nanotube (mwcnt) via Fischer esterification. *Arabian Journal for Science and Engineering* 35(1c): 37-48.

Azqhandi, M.H.A., Vasheghani, B.F., Rajabi, F.H. & Keramati, M. 2017. Synthesis of Cd doped ZnO/CNT nanocomposite by using microwave method: Photocatalytic behavior, adsorption and kinetic study. *Results in Physics* 7: 1106-1114.

Bell, T.E., Zhan, G., Wu, K., Zeng, H.C. & Torrente-Murciano, L. 2017. Modification of ammonia decomposition activity of ruthenium nanoparticles by N-doping of CNT supports. *Topics in Catalysis* 60(15): 1251-1259.

Chiang, Y.C., Lin, W.H. & Chang, Y.C. 2011. The influence of treatment duration on multi-walled carbon nanotubes functionalized by H2SO4/HNO3 oxidation. *Applied Surface Science* 257(6): 2401-2410.

Garzia, T., Marta, E.S., Palumbo, F., Palazzo, G., Giannossa, L.C., Mangone, A., Comparelli, R., Musso, S. & Favia, P. 2017. Towards highly stable aqueous dispersions of multi-walled carbon nanotubes: The effect of oxygen plasma functionalization. *Journal of Colloid and Interface Science* 491: 255-264.

Gopiraman, M., Ganesh Babu, S., Khatri, Z., Yoong, A.K., Endo, M., Karvembu, R. & Kim, I.S. 2013. An efficient, reusable copper-oxide/carbon-nanotube catalyst for N-arylation of imidazole. *Carbon* 62: 135-148.

Gui, M.M., Yap, Y.X., Chai, S.P. & Abdul Rahman, Mohamed. 2013. Amine-functionalization of multi-walled carbon nanotubes for adsorption of carbon dioxide. *Asia-Pacific Journal of Chemical Engineering* 8(2): 262-270.

Guo, T., Wu, J., Gao, H. & Chen, Y. 2017. Covalent functionalization of multi-walled carbon nanotubes with spiropyran for high solubility both in water and in non-aqueous solvents. *Inorganic Chemistry Communications* 83: 31-35.

Kanbur, Y. & Küçükyavuz, Z. 2011. Surface modification and characterization of multi-walled carbon nanotube. *Fullerenes, Nanotubes and Carbon Nanostructures* 19(6): 497-504.

Kharissova, O.V., Kharisov, B.I. & de Casas Ortiz, E.G. 2013. Dispersion of carbon nanotubes in water and non-aqueous solvents. *RSC Advances* 3(47): 24812-24852.

Kuroda, C., Haniu, H., Ajima, K., Tanaka, M., Sobajima, A., Ishida, H., Tsukahara, T., Matsuda, Y., Aoki, K., Kato, H. & Saito, N. 2016. The dispersion state of tangled multi-walled carbon nanotubes affects their cytotoxicity. *Nanomaterials* 6(11): 219.

Le, C.M.Q., Cao, X.T. & Lim, K.T. 2017. Ultrasound-promoted direct functionalization of multi-walled carbon nanotubes in water via Diels-Alder 'click chemistry'. *Ultrasonics Sonochemistry* 39: 321-329.

Lehman, J.H., Terrones, M., Mansfield, E., Hurst, K.E. & Meunier, V. 2011. Evaluating the characteristics of multiwall carbon nanotubes. *Carbon* 49(8): 2581-2602.

Ling, X., Wei, Y., Zou, L. & Xu, S. 2013. The effect of different order of purification treatments on the purity of multiwalled carbon nanotubes. *Applied Surface Science* 276: 159-166.

Liu, J., Zhao, G., Childers, D., Schweitzer, N., Marshall, C.L., Klie, R.F., Miller, J.T. & Meyer, R.J. 2014. Correlating the degree of metal-promoter interaction to ethanol selectivity over MnRh/CNTs CO hydrogenation catalysts. *Journal of Catalysis* 313: 149-158.

Ma, Q., Wang, D., Wu, M., Zhao, T., Yoneyama, Y. & Tsubaki, N. 2013. Effect of catalytic site position: Nickel nanocatalyst selectively loaded inside or outside carbon nanotubes for methane dry reforming. *Fuel* 108: 430-438.

Morsy, M., Helal, M., El-Okr, M. & Ibrahim, M. 2014. Preparation, purification and characterization of high purity multi-wall carbon nanotube. *Spectrochimica Acta Part A: Molecular and Biomolecular Spectroscopy* 132: 594-598.

Pistone, A., Ferlazzo, A., Lanza, M., Milone, C., Iannazzo, D., Piperno, A., Elpida, P. & Signorino, G. 2012. Morphological modification of MWCNT functionalized with HNO 3/H 2SO 4 mixtures. *Journal of Nanoscience and Nanotechnology* 12(6): 5054-5060.

Ren, X., Chen, C., Nagatsu, M. & Wang, X. 2011. Carbon nanotubes as adsorbents in environmental pollution management: A review. *Chemical Engineering Journal* 170(2): 395-410.

Sahebian, S., Zebarjad, S.M., Vahdati Khaki, J. & Lazzeri, A. 2016. The decoration of multi-walled carbon nanotubes with nickel oxide nanoparticles using chemical method. *International Nano Letters* 6(3): 183-190.

Santangelo, S., Messina, G., Faggio, G., Abdul Rahim, S.H. & Milone, C. 2012. Effect of sulphuric-nitric acid mixture composition on surface chemistry and structural evolution of liquid-phase oxidised carbon nanotubes. *Journal of Raman Spectroscopy* 43(10): 1432-1442.

Tatsuru, S., Yohei, N., Taibou, Y., Junko, H., Nagahiro, S., Osamu, T., Akiharu, T., Kazuhiro, N. & Youji, O. 2013. Functionalization of multiwalled carbon nanotubes by solution plasma processing in ammonia aqueous solution and preparation of composite material with polyamide 6. *Japanese Journal of Applied Physics* 52(12R): 125101.

Tessonnier, J.P., Rosenthal, D., Girgsdies, F., Amadou, J., Begin, D., Pham-Huu, C., Sheng, D.S. & Schlogl, R. 2009. Influence of the graphitisation of hollow carbon nanofibers on their functionalisation and subsequent filling with metal nanoparticles. *Chemical Communications* 46: 7158-7160.

Wang, S., Xin, Z., Huang, X., Yu, W., Niu, S. & Shao, L. 2017. Nanosized Pd-Au bimetallic phases on carbon nanotubes for selective phenylacetylene hydrogenation. *Physical Chemistry Chemical Physics* 19(8): 6164-6168.

Xiao, X., Sheng, Z., Yang, L. & Dong, F. 2016. Low-temperature selective catalytic reduction of NOx with NH3 over a manganese and cerium oxide/graphene composite prepared by a hydrothermal method. *Catalysis Science & Technology* 6(5): 1507-1514.

Zhang, J., Zou, H., Qing, Q., Yang, Y., Li, Q., Liu, Z., Guo, X. & Du, Z. 2003. Effect of chemical oxidation on the structure of single-walled carbon nanotubes. *The Journal of Physical Chemistry B* 107(16): 3712-3718.

Zhou, L., Forman, H., Yi, G. & Lunec, J. 2017. Multi-walled carbon nanotubes: A cytotoxicity study in relation to functionalization, dose and dispersion. *Toxicology in Vitro* 42: 292-298.

School of Chemical Engineering
Universiti Sains Malaysia
14300 Nibong Tebal, Pulau Pinang
Malaysia

*Corresponding author; email: chrahman@usm.my

Received: 19 September 2018
Accepted: 19 March 2019